Superlattices and Microstructures 54 (2013) 61–70

Contents lists available at SciVerse ScienceDirect

Superlattices and Microstructures

journal homepage: www.elsevier.com/locate/superlattices

Electron states and related optical responses in asymmetric inverse parabolic quantum wells

C.A. Duque [a,*], M.E. Mora-Ramos [a,b]

[a] Instituto de Física, Universidad de Antioquia, A.A. 1226, Medellín, Colombia
[b] Facultad de Ciencias, Universidad Autónoma del Estado de Morelos, Av. Universidad 1001, CP 62209 Cuernavaca, Morelos, Mexico

ARTICLE INFO

Article history:
Received 16 September 2012
Accepted 19 October 2012
Available online 6 November 2012

Keywords:
Quantum well
Nonlinear optics
Modulation doping
Electronic states

ABSTRACT

The article reports the obtention of the conduction band energy states for electrons in a Al_xGa_{1-x} As-based quantum well with inverse parabolic confinement. Accordingly, it has been possible to calculate the intersubband electron-transition-related optical absorption and rectification coefficients. The comparison between the results in the cases of symmetric and asymmetric rectangular barrier configurations allows to verify the possibility of the second-order optical rectification in the asymmetric case as well as a rather drastic change in the absorption coefficient as a function of the height of the inverse parabolic potential in such a configuration.

1. Introduction

The suitable use of crystal growth techniques allows the tailoring of the conduction and valence band profiles in semiconducting heterojunction systems. The incorporation of dopants results in the formation of high-density carrier gases and the band profiles become renormalized due to the many-body effects that can be theoretically accounted for by using self-consistent descriptions. The particular shape of the potential energy profile in this case changes with the application of the so-called modulation doping [1,2]; but very limited geometrical heterostructure potential configurations are achieved by this way. A more successful approach in this direction is the one known as compositional grading (for early reports see, for instance, [3–5] and references therein). Works dealing with different properties of compositionally graded heterojunctions have continued appearing throughout the years, and it is possible to refer a few as examples [6–11].

* Corresponding author. Tel.: +57 4 219 56 30; fax: +57 4 233 01 20.
E-mail address: cduque@fisica.udea.edu.co (C.A. Duque).

0749-6036/$ - see front matter © 2012 Elsevier Ltd. All rights reserved.
http://dx.doi.org/10.1016/j.spmi.2012.10.004

The use of compositional grading would allow the practical realization of semiconductor quantum confined quasi-two-, -one-, and -zero-dimensional nanosystems, with non-abrupt interfaces and/or with functional position-dependence of the conduction and valence band potential energy profiles. The possibility of designing specific confining potential shapes paves the way for the suitable tuning of different physical properties which can become the fundamentals of electronic and optoelectronic device applications. The semiconducting zincblende alloy $Al_xGa_{1-x}As$ reveals as one of the most promising materials for the obtention of this kind of heterosystems given the high degree of Al composition controlling achieved in nowadays crystal growth technologies, its direct bandgap regime up to $x = 0.45$ and the wide knowledge about its basic properties already attained.

Among the different possible profile configurations one finds the inverse parabolic one [12–19]. $Al_xGa_{1-x}As$-based heterostructures with inverse parabolic confinement have been the subject of the study of several optical nonlinearities in recent years [17,18]. In this paper, we are aimed at studying the nonlinear optical absorption and optical rectification related with intersubband electron transitions in a $Al_xGa_{1-x}As$ inverse parabolic quantum well (QW) with asymmetric rectangular potential barrier geometry. The purpose is to investigate the influence of the asymmetric confinement in the light absorption and the occurrence of second-order optical rectification. In accordance, the work is organized as follows: Section 2 will briefly present the theoretical framework of the study. Section 3 is devoted to discuss the obtained results and, finally, Section 4 contains the conclusions of the work.

2. Theoretical framework

Ref. [18] contains a detailed description of the model used in the calculation of the single electron states in the conduction band of the inverse parabolic QW. The authors consider the effective mass and parabolic band approximations. The main differences between our calculation and that reported in [18] are that we are not including external electric field effects and that the conduction band confining potential function now corresponds to an asymmetric barrier geometry:

$$V(z) = \begin{cases} V_1, & z < -L/2 \\ \frac{V_1}{\sigma}\left(1 - \left(\frac{2z}{L}\right)^2\right), & |z| \leqslant L/2 \\ V_2, & z > +L/2. \end{cases} \tag{1}$$

The quantity $\sigma = x_l/x_c$, where x_l is the value of the Al concentration in the left-hand barrier and x_c is the Al concentration at the QW center (in our particular asymmetric configuration we are assuming $V_1 > V_2$). Besides, L represents the well width.

The way of obtaining the single particle wavefunctions relies in a method developed by Xia and Fan [20], which was posteriorly used in the calculation of optical absorption in superlattices under magnetic fields by de Dios Leyva and Galindo [21]. Such an approach is based on the expansion of the electron states over a complete orthogonal basis of sine functions associated with a QW of infinite potential barriers with a width taken as $L_\infty = 50$ nm. Consequently, the z-dependent eigenfunctions of the effective mass Schrödinger-like conduction band Hamiltonian, with the potential given in Eq. (1) are written as

$$\phi(z) = \left(\frac{2}{L_\infty}\right)^{\frac{1}{2}} \sum_{n=1}^{\infty} C_n \sin\left(\frac{n\pi z}{L_\infty} + \frac{n\pi}{2}\right). \tag{2}$$

This is a pretty much realistic approach to the calculation of the confined electron states given that actual QW heterostructures do not contain infinite width potential barriers. Of course, the number of terms included in the calculation can neither be infinite. The convergence of Eq. (2), for the specific width of the QW considered, is ensured until 10^{-3} meV with the incorporation of 200 terms in the expansion of the $\phi(z)$ wavefunctions.

The optical coefficients to be evaluated are [22]: the absorption one, with its maximum resonant peak value given by;

$$\alpha_{\max} = \frac{e^2 N \omega_{01} M_{01}^2 T_1}{\hbar \varepsilon_0 c n}, \tag{3}$$

and the second-order optical rectification coefficient, with is maximum peak amplitude;

$$\chi_{0,max} = \frac{2e^3 N M_{01}^2 |M_{00} - M_{11}| T_0 T_1}{\varepsilon_0 \hbar^2}. \tag{4}$$

In these expressions, ε_0 is the vacuum permittivity, c is the speed of light in vacuum, n is the refractive index, and N is the electron density in the QW. In addition, $\omega_{01} = (E_1 - E_0)/\hbar$is the frequency value corresponding to the $0 \leftrightarrow 1$ intersubband transition, whilst $M_{ij} = \langle \phi_i | z | \phi_j \rangle$. The quantities T_0 and T_1 are the lifetimes of the electron in the ground and first excited states respectively. They are associated with damping mechanisms in the system and will be taken as input parameters in the calculation with fixed values: $T_0 = 1$ ps, and $T_1 = 0.2$ ps [18,23].

The values of the left- and right-hand potential barrier heights come from the application of the 60:40 band-offset rule to the energy bandgap differences at the $z = -L/2$ and $z = +L/2$ interfaces. We have used the compositional dependence of the $Al_xGa_{1-x}As$ energy gap as $E_g(x) = (1519 + 1155\, x + 370\, x^2)$ meV. The Al molar fraction corresponding to the left-hand barrier is, in our case, $x_l = 0.3$. In order to simplify the problem, we have taken homogeneous values of both the electron effective mass and dielectric constant throughout the whole structure. Given that x is small enough, the numerical differences that can be introduced via the inclusion of mechanical and dielectric mismatches are, in fact, negligible. In consequence, the calculation procedure considers the corresponding GaAs values: $m_e = 0.067 m_0$ (m_0 being the electron free mass) and $\varepsilon = n^2 = 12.5$.

3. Results and discussion

Fig. 1 contains our results for the energies of the lowest four electron states in the inverse parabolic QW with rectangular barriers in the symmetric barrier configuration. Fig. 1a shows these quantities as functions of the QW width for $x_c = x_l$, and Fig. 1b depicts the functional dependence of the energies on the height of the inverse parabolic potential at the QW center, for $L = 20$ nm. The horizontal dashed line indicates the energy position of the left-hand barrier top, V_0.

One may readily see that, as expected, the energies corresponding to the considered levels are decreasing functions of the QW width. However, in this symmetric case, the range of L reported guarantees that only the first two confined states actually belong to the inverse parabolic structure (although for narrow enough wells ($L \leqslant 8$ nm), there is only one). The higher ones appear as a result of the influence of the infinite barriers put at $\pm L_\infty/2$ for the sake of the calculation tool. That is why the decrease observed for them is much less pronounced.

Keeping the symmetric QW geometry but reducing the height of the central parabolic barrier, V_h, it is possible to confine the four lowest states allowed within the parabolic well region. All these quantities are increasing functions of the central barrier height. By augmenting V_h the upper levels are progressively removed from the parabolic QW. It is also possible to notice that when $V_h \simeq V_1 = V_0$ and the QW is sufficiently wide, the ground state becomes degenerated, with the energy E_0 corresponding to two different states in a double quasi-triangular QW. This is due to the effect of the central barrier that uncouples the left and right potential wells.

The energy levels that correspond to the asymmetric barrier ($V_2 = V_0/2$) geometry appear depicted in Fig. 2. First, Fig. 2a shows these levels as functions of the QW width for a fixed parabolic central barrier height $V_h = V_0/4$. Then, in Fig. 2b we present these quantities as functions of V_h when L is fixed at 20 nm.

As expected, the QW confined energies are now lower. According to Fig. 2a, if L lies below 3 nm, not a single electron state confines within the inverse parabolic QW level; and in the range of widths reported, there will be –again, at most– two electronic levels belonging to our active QW region. However, now the asymmetry prevents the degeneracy of the ground state when L becomes large.

With a fixed QW width, the variation of V_h implies the growth in the E_j, ($i = 0, \ldots, 3$), but in this case the asymmetric QW is only able to confine the first three states when the central parabolic barrier

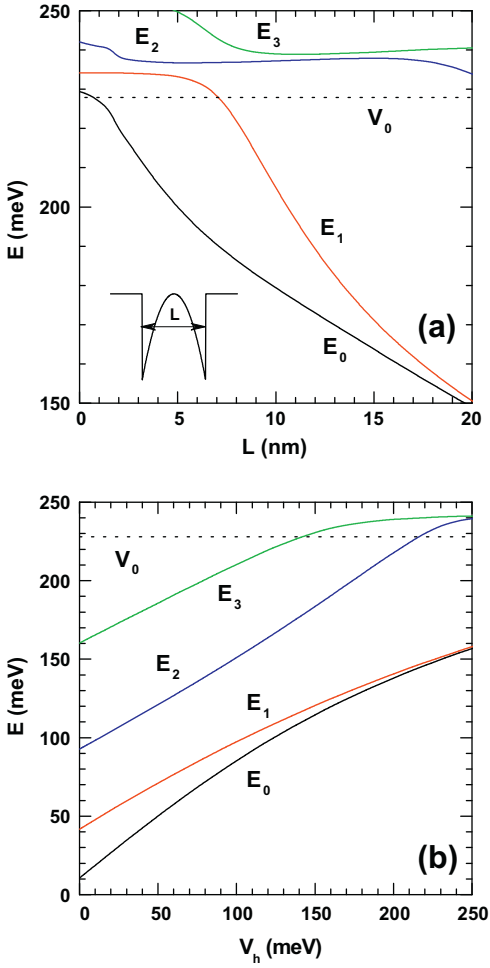

Fig. 1. Energies of the lowest four states for a rectangular quantum well plus inverted central parabolic quantum well with symmetric potential barriers. In (a) the results are as a function of the well width for a fixed value of the central potential barrier: $V_h = V_0$. In (b) the results are as a function of the height of the central inverted parabolic barrier for fixed values of the quantum well width: $L = 20$ nm.

height is small enough. The progressive increase in V_h up to the value of the right-hand rectangular barrier can only lead to the occurrence of a single confined state, the ground one, whereas the higher levels are pushed upwards to the region of energies confined by the infinite QW of width L_∞.

To help understanding the optical properties presented below, we show in Figs. 3 and 4 the calculated coefficients M_{01}^2 and $|M_{00} - M_{11}|$ in the symmetric and asymmetric inverse parabolic QW configurations respectively.

From Fig. 3 we directly observe that the symmetry leads to the vanishing of intrasubband matrix elements M_{ii} ($i = 0,1$). Therefore, we verify that no second-order optical rectification is achieved in symmetric inverse parabolic QWs with rectangular barriers. The square of the intersubband matrix element, M_{01}, has a mixed behavior as the result of the growth in the QW width. Initially, when $L = 0$, this element has its largest value, which corresponds to the expected value of the z-position between states that extend from $-L_\infty/2$ to $+L_\infty/2$. Then, as long as the QW augments, this element will represent, first, the expected value of the electron position between the ground state confined within

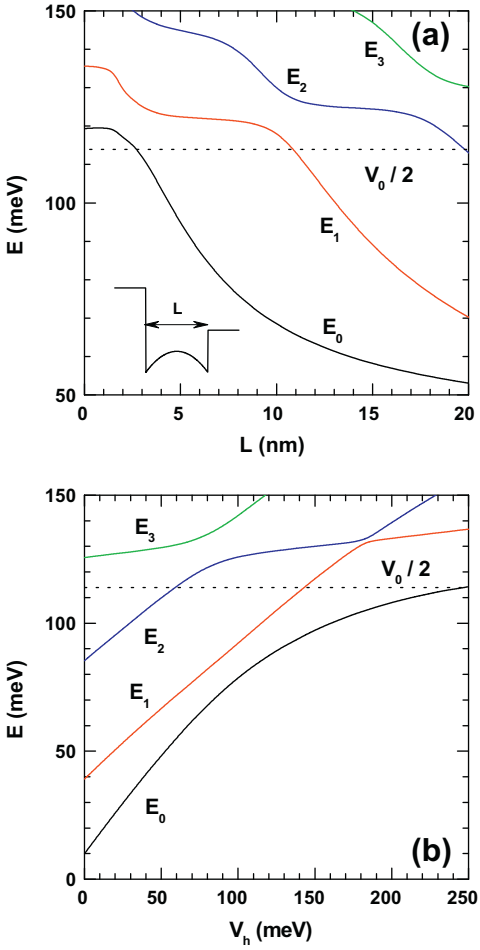

Fig. 2. Energies of the lowest four states for an asymmetric rectangular quantum well ($V_1 = V_0$ and $V_2 = V_0/2$) plus inverted central parabolic potential barrier. In (a) the results are as a function of the well width for a fixed value of the central potential barrier: $V_h = V_0/4$. In (b) the results are as a function of the height of the central inverted parabolic barrier for fixed values of the quantum well width: $L = 20$ nm.

the QW and the first excited state confined by the external infinite well. Since the ground state wavefunction is spatially localized inside the well, this expected value diminishes. But, as long as the width L augments the ground state wavefunction spreads over a wider region and the first excited one becomes localizes in the well, provided the level E_1 confines in it. The overlap between the two wavefunctions strengthens and the intersubband expected value of the electron position starts to rise. The further widening of the QW leads to the degeneracy of the ground state. In this situation, the electron probability density will have two well defined maxima centered at the quasi-rectangular –almost uncoupled– wells. Therefore, the larger values of z will be those that greatly contribute to the expected electron position value.

Observing Fig. 3b, it is possible to give a similar explanation for the increasing variation of $|M_{01}|^2$ as a function of V_h when the well width keeps fixed. The larger the height of the parabolic central barrier, the more defined the double quasi-triangular QW geometry. In consequence, the main contribution to the electron position expected value comes from the bigger z-values –in positive and negative directions– inside the QW.

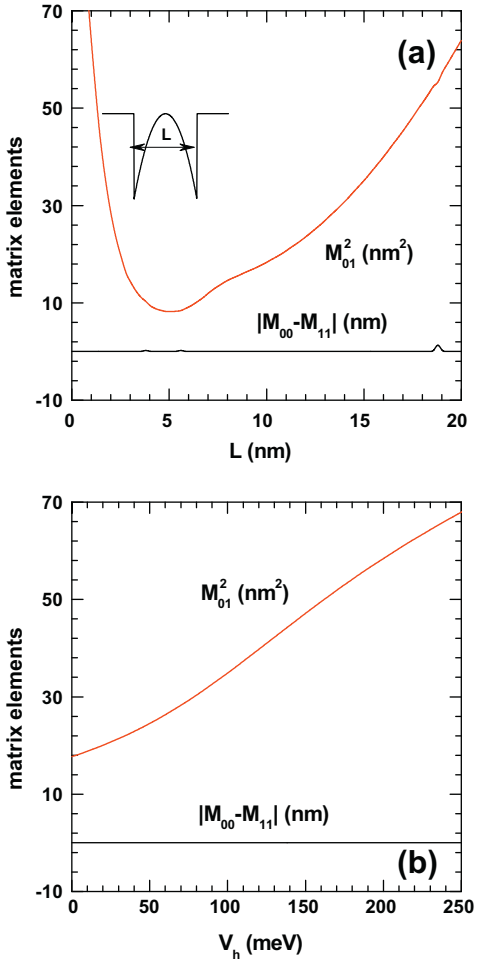

Fig. 3. Involved matrix elements for a rectangular quantum well plus inverted central parabolic quantum well with symmetric potential barriers. In (a) the results are as a function of the well width for a fixed value of the central potential barrier: $V_h = V_0$. In (b) the results are as a function of the height of the central inverted parabolic barrier for fixed values of the quantum well width: $L = 20$ nm.

For the asymmetric inverse parabolic QW the situation for the dipole matrix elements is somewhat different; but can be explained straightforwardly with the help of the results given in Fig. 2 for the energy levels. First, we readily notice that the term $|M_{00} - M_{11}|$ is, in general, distinct from zero. It vanishes if $L = 0$ because that is the limit of a symmetric infinite QW and both intrasubband matrix elements become null. There is also another value at which the absolute difference vanishes (at $L \simeq 13.5$ nm). In such case, the ground and first excited states confine within the QW region. Then, what happens is that the expected value of the electron position becomes the same for both levels. Otherwise, one notices that there is an increment in the term when the well width augments from zero to approximately 7 nm, and then it begins to diminish. If one observes Fig. 2a, it becomes clear that the initial increase comes from the combination of the progressive localization of the ground state and the fact that the first excited one spreads over the region $z \in [-L/2, +L_\infty/2]$. Then, the expected value M_{11} is progressively larger than M_{00}. Going above $L \simeq 5$ nm, the value of the squared difference remains practically constant because the energy E_1 changes very little –although diminishes. The

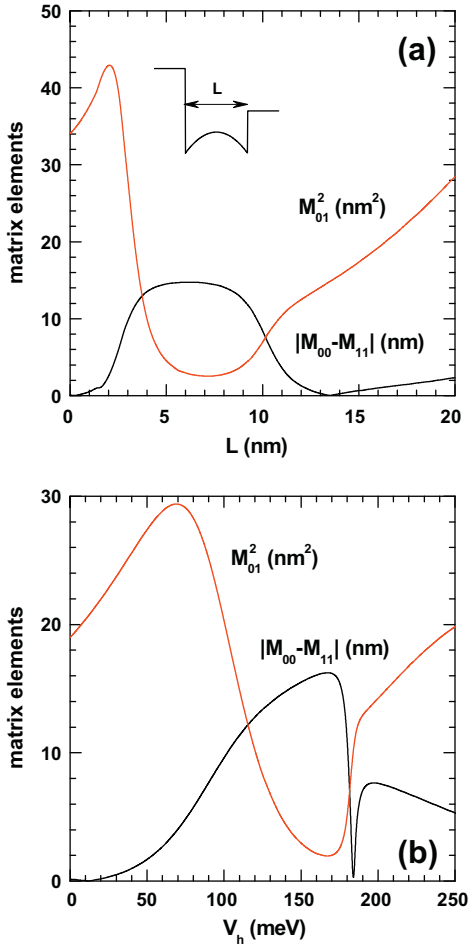

Fig. 4. Involved matrix elements for a asymmetric rectangular quantum well ($V_1 = V_0$ and $V_2 = V_0/2$) plus inverted central parabolic quantum well. In (a) the results are as a function of the well width for a fixed value of the central potential barrier: $V_h = V_0/4$. In (b) the results are as a function of the height of the central inverted parabolic barrier for fixed values of the quantum well width: $L = 20$ nm.

reduction when $L \gtrsim 8$ nm comes from the fall in E_1, and turns to be more abrupt after this energy level becomes confined by the inverse parabolic QW because $|\phi_1(z)|^2$ mostly lies within the QW region.

The intersubband squared matrix element $|M_{01}|^2$ behaves much alike the symmetric case, with the exception of the lowest L interval where it exhibits a rather sharp increase. It should be noticed that, in that region, both E_0 and E_1 correspond to extended states of the external infinite well and, as soon as the ground state becomes confined by the inverse parabolic well, the magnitude of M_{01} stops raising and initiates a sharp decrease.

Analyzing the dependence of these two matrix element coefficients with respect to the variation of the height of the central parabolic barrier [Fig. 4b], it is seen that the shape of the $|M_{01}|^2$ curve pretty much resembles that of its corresponding one in Fig. 4a; but now, the justification is somewhat distinct. The initial increase observed for $V_h \in [0,70]$ meV obeys to the fact that the first excited state (localized within the QW or not) and the ground state shift upwards pushed by the rise of the QW bottom. Therefore, the corresponding wavefunctions spread over a larger coordinate interval and the value of the intersubband matrix element of the electron position grows. The fall observed between 70

meV and ∼160 meV is due to the fact that augmenting V_h in such range implies that whilst $|\phi_0(z)|^2$ remains confined in the QW, the electron density of probability that corresponds to the first excited state spreads towards the right-hand infinite barrier, a region where the ground state probability density is very small. The further rise in $|M_{01}|^2$ relates with the enhancement of the spatial extension of the ground state, pushed upwards by the central barrier. One may also see an abrupt change in the slope of this curve at the value of V_h where there is an anti-crossing of the first and second excited states (in the infinite well region of confinement). This phenomenon is confirmed by noticing that the value of $|M_{00} - M_{11}|$ is almost equals to zero at that point, which is related to the fact that the two states acquire very similar electron density distributions (notice that for such a value of V_h, the ground state lies close to the right-hand barrier top).

Nonetheless, the range of V_h values of actual interest in regard with the coefficients of optical absorption and nonlinear optical rectification is $V_h \in [0, \approx 140\ \text{meV}]$. This is because we shall only have the ground and first excited states confined within the QW in such an interval. It is directly seen

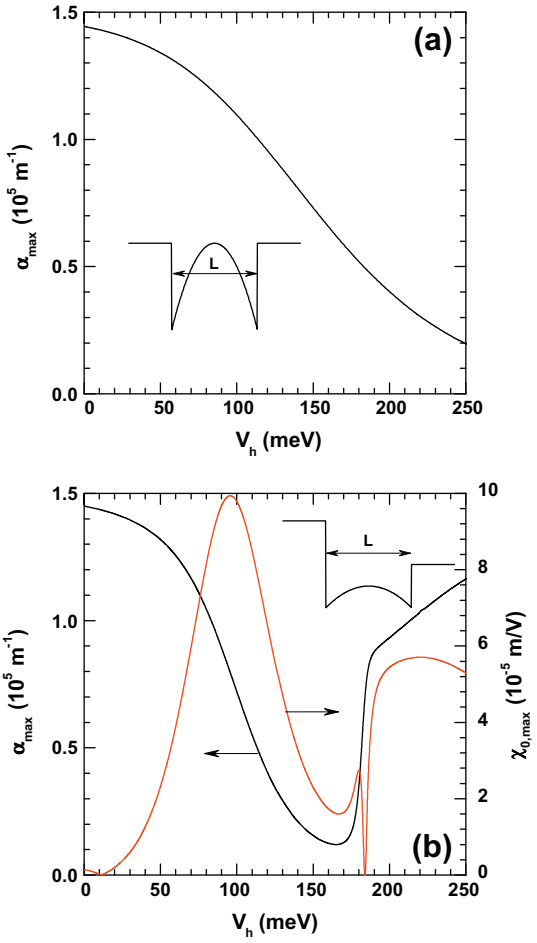

Fig. 5. Resonant peak of the nonlinear optical absorption (α_{max}) and nonlinear optical rectification ($\chi_{0,max}$) in a symmetric rectangular quantum well ($V_1 = V_2 = V_0$) (a) and asymmetric rectangular quantum well ($V_1 = V_0$ and $V_2 = V_0/2$) (b) plus inverted central parabolic quantum well. The results are as a function of the height of the central inverted parabolic barrier for fixed values of the quantum well width: $L = 20$ nm.

from Fig. 5 that the rectification coefficient has a maximum peak amplitude at a value where, according to Fig. 4b, there will the maximum contribution from the product $|M_{01}|^2|M_{00} - M_{11}|$.

On the other hand, the maximum peak amplitude of the optical absorption coefficient shows a decreasing behavior as a function of the height of the central parabolic barrier in the symmetric and the asymmetric QW geometries as a result of the combination of the functional dependencies of $|M_{01}|^2$ and ω_{01} with respect to V_h (we see, for instance, that in the symmetric case $E_1 - E_0$ decreases also when v_h augments).

With respect to the magnitude, it can be noticed that the values obtained for $\alpha_{\max}$ are of the same order of magnitude than the ones reported by Kasapoglu et al. [18] in the case of a symmetric inverse parabolic QW with an applied electric field–although with a narrower well width.

4. Conclusions

In this work we have studied the properties of the electron states in Al_xGa_{1-x} As-based inverse parabolic quantum wells, making emphasis in the asymmetric configuration with rectangular potential barriers. The results show the dependence of the positions of the energy levels confined within the well region as functions of its width and the height of the inner inverse parabolic barrier. This geometry allows, in principle for the appearance of intersubband electron-related optical responses like the nonlinear optical rectification, without the need, for instance, of the application of external probes like an electric field.

However, since the asymmetric system can accommodate less confined levels, there is a wider range of central barrier heights in which –compared with the symmetric quantum well case– no intersubband transition occurs and the optical responses considered are not present. But in the particular configurations where these transitions between the confined ground and first excited are possible, the magnitude of the optical rectification peak is more than order of magnitude larger than its corresponding one in –for example– asymmetric Pöschl-Teller quantum wells [24]; and of the same order of magnitude than $\chi_{0,\max}$ in the case of exciton-related nonlinear optical rectification in asymmetric cylindrical quantum dots under the influence of an external electric field [25]. Therefore, we may conclude that a compositionally graded heterostructure like the inverse parabolic QW could find application as an optical rectifier.

Acknowledgments

This research was partially supported by the Colombian Agencies COLCIENCIAS, CODI-Universidad de Antioquia (project: E01535-Efectos de la presión hidrostática y de los campos eléctrico y magnético sobre las propiedades ópticas no lineales de puntos, hilos y anillos cuánticos de GaAs-(Ga,Al)As y Si/SiO_2), and Facultad de Ciencias Exactas y Naturales–Universidad de Antioquia (CAD-exclusive dedication Project: 2012–2013). M.E.M.R thanks Mexican CONACYT for support through 2012-2013 sabbatical Grant No. 180636 as well as Research Grant CB-2008-101777. He is also grateful to the Universidad de Antioquia and the Escuela de Ingeniería de Antioquia for hospitality during his sabbatical stay.

References

[1] R. Dingle, H.L. Störmer, A.C. Gossard, W. Wiegmann, Appl. Phys. Lett. 33 (1978) 665.
[2] E.F. Schubert, L.W. Tu, G.J. Zydzik, R.F. Kopf, A. Benvenuti, M.R. Pinto, Appl. Phys. Lett. 60 (1992) 466.
[3] L.J. Van Ruyven, Annu. Rev. Mater. Sci. 2 (1972) 501.
[4] L.M. Roth, A.J. Bennet, Phys. Rev. B 6 (1972) 2238.
[5] F. Capasso, Science 235 (1987) 172.
[6] J.R. Waldrop, S.P. Kowalczyk, R.W. Grant, E.A. Kraut, D.L. Miller, J. Vac. Sci. Technol. 19 (1981) 573.
[7] M. Sundaram, A.C. Gossard, J. Appl. Phys. 73 (1993) 251.
[8] S. Vlaev, F. García-Moliner, V.R. Velasco, Phys. Rev. B 52 (1995) 13784.
[9] H. Sari, E. Kasapoglu, I. Sokmen, Physica B 325 (2003) 300.
[10] E. Kasapoglu, I. Sökmen, Physica B 403 (2008) 3746.
[11] G.F. Brown, J.W. Ager, W. Walukiewicz, J. Wu, Sol. Energ. Mat. Sol. Cells 94 (2010) 478.
[12] W.Q. Chen, S.M. Wang, T.G. Andersson, J.T. Thordson, Phys. Rev. B 48 (1993) 14264.

[13] W.Q. Chen, S.M. Wang, T.G. Andersson, J.T. Thordson, J. Appl. Phys. 74 (1993) 6247.
[14] S. Vlaev, V.R. Velasco, F. García-Moliner, Phys. Rev. B 51 (1995) 7321.
[15] S. Baskoutas, A.F. Terzis, Physica E 40 (2008) 1367.
[16] S. Baskoutas, A.F. Terzis, Eur. Phys. J.B 69 (2009) 237.
[17] S. Baskoutas, C. Garoufalis, A.F. Terzis, Eur. Phys. J.B 84 (2011) 241.
[18] F. Ungan, U. Yesilgul, E. Kasapoglu, H. Sari, I. Sökmen, J. Lumin. 132 (2012) 1627.
[19] E.C. Niculescu, Eur. Phys. J.B 85 (2012) 66.
[20] J.-B. Xia, W.-J. Fan, Phys. Rev. B 40 (1989) 8508.
[21] M. de Dios Leyva, V. Galindo, Phys. Rev. B 48 (1993) 4516.
[22] M. Załużny, Phys. Rev. B 47 (1993) 3995.
[23] J.C. Martínez-Orozco, M.E. Mora-Ramos, C.A. Duque, J. Lumin. 132 (2012) 449.
[24] S. Şakiroğlu, F. Ungan, U. Yesilgul, M.E. Mora-Ramos, C.A. Duque, E. Kasapoglu, H. Sari, İ. Sökmen, Phys. Lett. A 376 (2012) 1875.
[25] R.E. Acosta, A. Zapata, C.A. Duque, M.E. Mora-Ramos, Physica E 44 (2012) 1936.